

Non-volatile multi-state magnetic domain transformation in a Hall balance

Yang Gao(高阳), Jingyan Zhang(张静言), Pengwei Dou(窦鹏伟), Zhuolin Li(李卓霖), Zhaozhao Zhu(朱照照), Yaqin Guo(郭雅琴), Chaoqun Hu(胡超群), Weidu Qin(覃维都), Congli He(何聪丽), Shipeng Shen(申世鹏), Ying Zhang(张颖), and Shouguo Wang(王守国)

Citation: Chin. Phys. B, 2022, 31 (**6**): 067502. DOI: 10.1088/1674-1056/ac65f5
Journal homepage: http://cpb.iphy.ac.cn; http://iopscience.iop.org/cpb

What follows is a list of articles you may be interested in

Exact soliton solutions in anisotropic ferromagnetic wires with Dzyaloshinskii-Moriya interaction

Qiu-Yan Li(李秋艳), Dun-Zhao(赵敦), and Zai-Dong Li(李再东)
Chin. Phys. B, 2021, 30 (**1**): 017504. DOI: 10.1088/1674-1056/abca26

Spin waves and transverse domain walls driven by spin waves: Role of damping

Zi-Xiang Zhao(赵梓翔), Peng-Bin He(贺鹏斌), Meng-Qiu Cai(蔡孟秋), Zai-Dong Li(李再东)
Chin. Phys. B, 2020, 29 (**7**): 077502. DOI: 10.1088/1674-1056/ab90e5

Lorentz transmission electron microscopy for magnetic skyrmions imaging

Jin Tang(汤进), Lingyao Kong(孔令尧), Weiwei Wang(王伟伟), Haifeng Du(杜海峰), Mingliang Tian(田明亮)
Chin. Phys. B, 2019, 28 (**8**): 087503. DOI: 10.1088/1674-1056/28/8/087503

Nonmonotonic effects of perpendicular magnetic anisotropy on current-driven vortex wall motions in magnetic nanostripes

Su Yuan-Chang, Lei Hai-Yang, Hu Jing-Guo
Chin. Phys. B, 2015, 24 (**9**): 097506. DOI: 10.1088/1674-1056/24/9/097506

Dynamics of magnetic skyrmions

Liu Ye-Hua, Li You-Quan
Chin. Phys. B, 2015, 24 (**1**): 017506. DOI: 10.1088/1674-1056/24/1/017506

RAPID COMMUNICATION

Non-volatile multi-state magnetic domain transformation in a Hall balance

Yang Gao(高阳)[1,2], Jingyan Zhang(张静言)[3,†], Pengwei Dou(窦鹏伟)[3], Zhuolin Li(李卓霖)[2], Zhaozhao Zhu(朱照照)[2,4], Yaqin Guo(郭雅琴)[1], Chaoqun Hu(胡超群)[1], Weidu Qin(覃维都)[1], Congli He(何聪丽)[1], Shipeng Shen(申世鹏)[1], Ying Zhang(张颖)[2,4,‡], and Shouguo Wang(王守国)[1,§]

[1] *Institute of Advanced Materials, Beijing Normal University, Beijing* 100875, *China*
[2] *Beijing National Laboratory for Condensed Matter Physics and Institute of Physics, Chinese Academy of Sciences, Beijing* 100190, *China*
[3] *School of Materials Science and Engineering, University of Science and Technology Beijing, Beijing 100083, China*
[4] *Songshan Lake Materials Laboratory, Dongguan* 523808, *China*

(Received 28 March 2022; revised manuscript received 3 April 2022; accepted manuscript online 11 April 2022)

High performance of the generation, stabilization and manipulation of magnetic skyrmions prompts the application of topological multilayers in spintronic devices. Skyrmions in synthetic antiferromagnets (SAF) have been considered as a promising alternative to overcome the limitations of ferromagnetic skyrmions, such as the skyrmion Hall effect and stray magnetic field. Here, by using the Lorentz transmission electron microscopy, the interconversion between the single domain, labyrinth domain and skyrmion state can be observed by the combined manipulation of electric current and magnetic field in a Hall balance (a SAF with the core structure of $[Co/Pt]_4/NiO/[Co/Pt]_4$ showing perpendicular magnetic anisotropy). Furthermore, high-density room temperature skyrmions can be stabilized at zero field while the external stimulus is removed and the skyrmion density is tunable. The generation and manipulation method of skyrmions in Hall balance in this study opens up a promising way to engineer SAF-skyrmion-based memory devices.

Keywords: magnetic skyrmion, Hall balance, electromagnetic coordinated manipulation, Lorentz transmission electron microscopy (LTEM)

PACS: 75.60.Ch, 75.50.Ee, 75.70.Cn, 68.37.Lp **DOI:** 10.1088/1674-1056/ac65f5

1. Introduction

Magnetic skyrmions with nontrivial vortex-like spin texture have attracted considerable attention for their fascinating physics and promising application.[1–4] The transformation between skyrmions and diverse magnetic domains has been proposed to construct low-energy-dissipation and multifunctional spintronic devices based on multi-state domains.[5] Bloch-type skyrmions were initially found in bulk B20 chiral magnets with large bulk Dzyaloshinskii–Moriya interaction (DMI).[2,6–8] Subsequently, skyrmions were also observed in magnetic films such as Fe/Ir,[9] Pt/Co,[10] and Pt/Co/Ta,[11,12] where the interfacial DMI played an important role to stabilize Néel-type skyrmions at room temperature by incorporating heavy metal layers with ferromagnetic (FM) layers. On the other hand, skyrmions in multilayers are notably favorable since the magnetic interactions can be easily engineered by stack sequences, layer thicknesses, repetition periods and external excitations.[13–15] Furthermore, the dynamic creation and driven behavior of skyrmions induced by the current have been investigated in multilayers theoretically[16–19] and experimentally,[12,20] laying a good foundation for future spintronic devices.

However, the main focus about skyrmions in magnetic films has been put on the FM multilayers, which suffer from the stray magnetic field and precessional dynamics, limiting the bit size[21] and operation speed.[22] Besides, the Magnus force acting on the FM skyrmions produces an extra lateral velocity in addition to the direction of the driving current, i.e., the skyrmion Hall effect (SkHE),[23,24] which hinders the application of skyrmions for the practical devices. Recently, above mentioned obstacles have been addressed by introducing skyrmions in antiferromagnetic (AFM) magnets due to their inhibited SkHE[25] and negligible stray fields.[26] In particular, the synthetic antiferromagnet (SAF) structures,[27,28] consisting of two FM layers separated by a spacer, have been considered to be a promising candidate to study AFM skyrmions due to the presence of interlayer DMI and perpendicular magnetic anisotropy (PMA).[29] The interfacial coupling type (FM or AFM) between the magnetic layers can be tuned by tailoring thicknesses of the spacer layers through the Ruderman–Kittel–Kasuya–Yosida (RKKY) interaction.[28] It has been demonstrated that high-density skyrmions can be successfully stabilized in a Hall balance,[30] (a SAF with FM layers showing PMA), while the controllable manipulation and multi-state transformation of magnetic textures in the Hall balance are still lacking.

[†]Corresponding author. E-mail: jyzhang@ustb.edu.cn
[‡]Corresponding author. E-mail: zhangy@iphy.ac.cn
[§]Corresponding author. E-mail: sgwang@bnu.edu.cn

© 2022 Chinese Physical Society and IOP Publishing Ltd

In this work, we demonstrated the non-volatile multi-state interconversion by electromagnetic coordinated manipulation in a Hall balance (core structure $[Co/Pt]_4/NiO/[Co/Pt]_4$). The transformation from the ground single domain to labyrinth domains via current injection was observed using Lorentz transmission electron microscopy (LTEM). Under a small magnetic field (60 Oe), a high-density skyrmion state can be formed when a certain density of current was applied. Furthermore, all the generated magnetic states can be stabilized at zero field and room temperature after removing the external excitations. The controllable magnetic states and skyrmion density at room temperature prompt the further nano-patterned design and application of skyrmions for storage devices based on Hall balance.

2. Experimental methods

The multilayered structures of $Pt(3)/[Co(0.4)/Pt(0.8)]_4/NiO/[Co(0.4)/Pt(0.8)]_4$ ($[Co/Pt]_4/NiO/[Co/Pt]_4$ for short, thickness in nm) were deposited simultaneously on the thermally oxidized Si wafers and Si_3N_4 membrane window via magnetron sputtering (AJA, ATC-2200). The thickness of the NiO layer was chosen as 1.3 nm to realize a moderate AFM coupling for top and bottom FM multilayers. The base pressure was better than 6×10^{-6} Pa, and the working argon pressure was 0.5 Pa. The multilayers on the thermally oxidized Si wafers were patterned into Hall bars with a channel width of 20 μm for the anomalous Hall effect (AHE) measurements. The films grown on the Si_3N_4 membrane windows were used for magnetic domain observation by LTEM (JEOL2100F). With the use of the Fresnel LTEM mode, the magnetic contrasts were imaged under the convergent or divergent electron beam at different focuses, which were introduced by the interaction of the electron beams with the in-plane magnetization. In order to observe the Néel-type magnetic domains, LTEM with simultaneous sample tilting was used to image the domain contrast. The perpendicular magnetic field was introduced by increasing the objective lens current. The skyrmion manipulation behavior by electric current was conducted using a double-tilt electrical TEM holder with two electrical conducting blocks at two sides of the film. A current pulse with 150 μs pulse width was supplied by a source-measure unit instrument (Keithley 6221).

3. Results and discussion

A Hall balance with a core structure of $[Co/Pt]_4/NiO/[Co/Pt]_4$ is shown schematically in Fig. 1(a). The interlayer exchange coupling (IEC) or RKKY coupling between the FM layers has been demonstrated to be highly tunable and oscillates with the thickness of NiO in the previous studies.[28,30] The FM coupling for top and bottom $[Co/Pt]_4$ layers can be achieved when NiO is chosen to 1.0–1.1 nm and 1.4–1.5 nm, while two FM multilayers exhibit AFM coupling at 1.2–1.3 nm. In this study, a Hall balance with AFM coupling (NiO thickness $\sim$ 1.3 nm) was used to investigate the magnetic domain structures as well as their evolution under multi-field manipulation. Figure 1(b) shows the AHE loops with multiple configurations, where the high and low values of Hall resistivity result from the parallel and antiparallel alignments of two perpendicular $[Co/Pt]_4$ FM layers, respectively. Figure 1(c) presents the under-focus LTEM image of the sample under a tilting angle of $-15°$ along the incident electron plane. The LTEM results indicate an AFM state without magnetic domain contrast, which coordinates with the antiparallel ground state in Fig. 1(b). The antiparallel single domain state can persist under the perpendicular magnetic field of 300 Oe (Fig. 1(d)) and no transformation of the single domain state was observed in the process of applying magnetic fields. When the external field was removed at a strength (1000 Oe) larger than the saturated field (650 Oe), the remnant state of the sample was still a single domain state. In contrast, the ground states or remnant states in FM multilayers such as Pt/Co/Ta mainly show labyrinth-shape domains and transform into the scattered skyrmion state under perpendicular magnetic fields, which results from the competition among the ferromagnetic exchange interaction, perpendicular magnetic anisotropy, interfacial DMI and external magnetic fields.[11,12] Furthermore, it has been demonstrated that large PMA limits the formation of high-density skyrmions whether in the FM or SAF multilayers and the electromagnetic coordinated method can be used as an efficient method to manipulate the topological magnetic domains.[11,12,31]

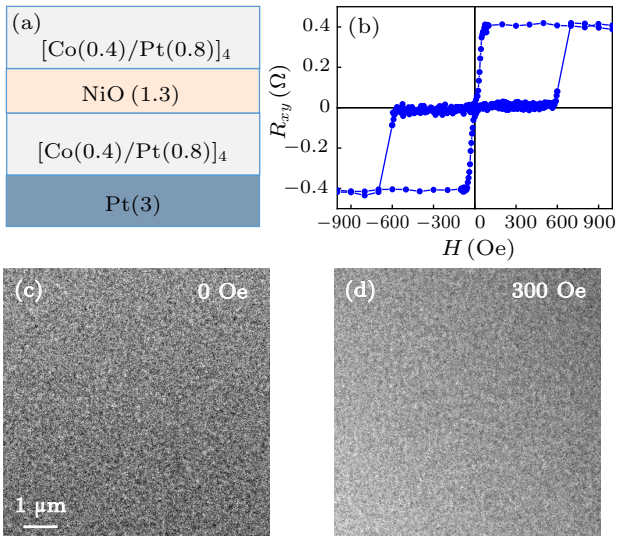


Fig. 1. (a) Hall balance with a core structure of $Pt(3)/[Co(0.4)/Pt(0.8)]_4/NiO(1.3)/[Co(0.4)/Pt(0.8)]_4$ (thickness in nm). (b) AHE loop for the Hall balance. Under-focus LTEM images for a Hall balance under the perpendicular magnetic field of (c) 0 and (d) 300 Oe (the scale bar is 1 μm).

Currently, the focus will be given on the domain evolution with the influences of electric current. A current pulse with 150 μs width was applied to the sample, as illustrated in Fig. 2(a). Before applying the electric current, the sample was saturated under sufficient magnetic fields, and then

the fields were removed. Combined with the simultaneous LTEM observation, it is found that the sample keeps the remnant single domain until the current density J is increased to 2.19×10^8 A/m^2, then the scattered inversed domains can be observed when J reaches 3.02×10^8 A/m^2. As the current density is further increased, spiral domains emerge first at the corner and gradually expand to fill the whole region. Finally, the labyrinth domains appear with small size. Figures 2(b)–2(g) show the evolution of the magnetic domain structures under the electric current, indicating that the labyrinth domains can be generated at zero field. Previous studies have demonstrated that the electric current can create the skyrmions and enhance the skyrmion density in the asymmetric magnetic multilayers[12] and centrosymmetric alloy,[32,33] where the contribution of Joule heating by injected current plays a minor role. In our cases, electric current promotes the generation and propagation of the multi-domains state.[19,34–36,36,37]

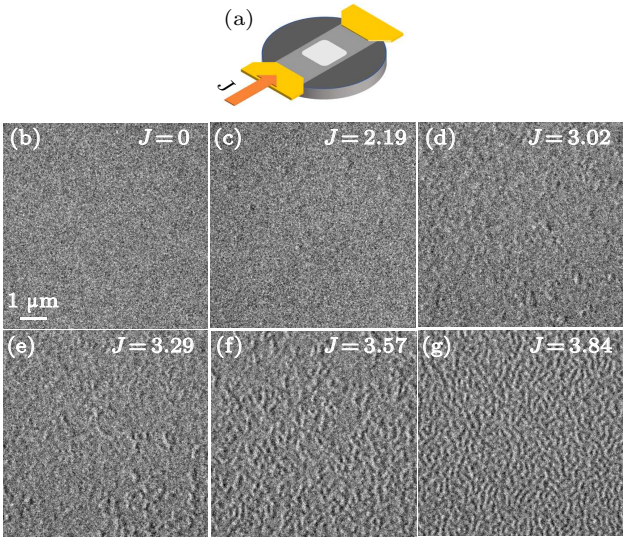


Fig. 2. Current manipulation of Hall balance from the saturation state. (a) Schematic geometry for LTEM imaging, where only the electric current was applied. Magnetic domain evolution at current densities of (b) $J = 0$, (c) $J = 2.19$, (d) $J = 3.02$, (e) $J = 3.29$, (f) $J = 3.57$ and (g) $J = 3.84$ ($\times 10^8$ A/m^2). The scale bar is 1 μm. Magnetic domain states persist after the removal of the electric current.

The generation of labyrinth domains rather than skyrmions by electric current alone shows that the labyrinth domains are hard to be pinched off without the assistance of magnetic fields. Therefore, the electromagnetic coordinated manipulation via simultaneously applying the magnetic field and electric current was performed in the Hall balance. The experimental procedure is that a perpendicular magnetic field with certain strength is applied first, followed by the injection of current pulse with a fixed current density. Then all the external stimuli are removed. The magnetic field dependence of domain evolution at a fixed current density of 3.84×10^8 A/m^2 is shown in Figs. 3(a)–3(f). The labyrinth domains keep unchanged under a magnetic field of 10 Oe after applying the current [Fig. 3(a)]. With increasing magnetic fields, the labyrinth domains gradually transform into skyrmions and the highest density skyrmion state takes place at a magnetic field of 57 Oe. The current density and magnetic field to produce the high-density skyrmions in the Hall balance are fairly smaller than those in other multilayers.[12,31] When further increasing magnetic fields, the density of skyrmions gradually decreases. The skyrmions can be identified as Néel-type in the Hall balance based on their response to a tilting angle, where the skyrmion type is invariant with respect to external magnetic fields although the density varies. The magnetic field dependence of the skyrmion density extracted from LTEM images is summarized in Fig. 3(g). It shows that the skyrmion density decreases linearly with magnetic fields after reaching its peak at 57 Oe. As a suitable magnetic field will cut off the helical or spiral ground state to form skyrmions in most bulk or film samples,[7,11] the small magnetic field plays a role to break off the labyrinth domains in the Hall balance. Those results clearly indicate that high-density skyrmions in Hall balance can be properly generated by applying an electric current with the assistance of a moderate magnetic field, which is beneficial to the device application.

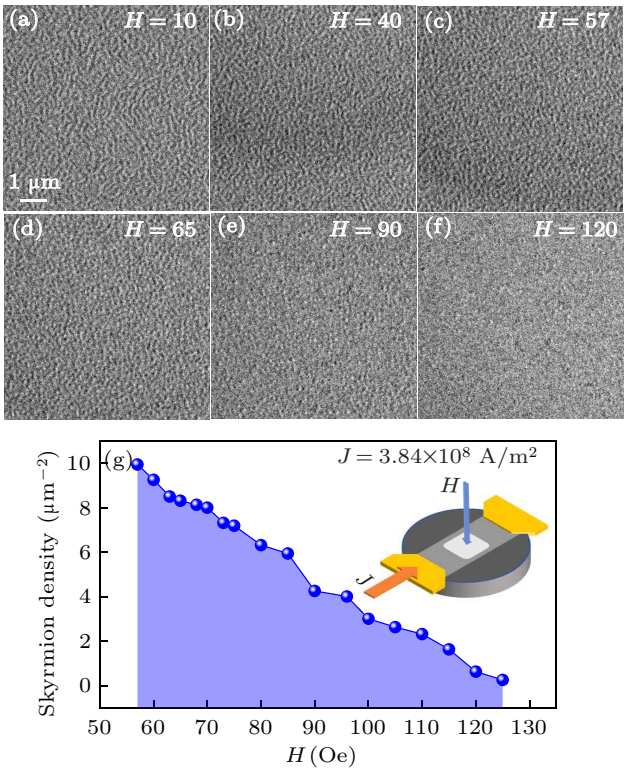


Fig. 3. Electromagnetic coordinated manipulation of Hall balance with a fixed electric current. (a)–(f) LTEM images of domain evolution via applying a fixed current density of $J = 3.84 \times 10^8$ A/m^2 under a perpendicular magnetic field (a) from 10 Oe to (f) 120 Oe. The scale bar is 1 μm. (g) Skyrmion density distribution as a function of magnetic field.

Based on the evolution of magnetic domains by the electromagnetic coordinated manipulation, the single domain, labyrinth domain and skyrmion states can be generated via certain manipulation conditions. It should be noted that all the magnetic states persist after the removal of external stimuli including electric current and magnetic field. Figure 4 shows the

interconversion of single domain, labyrinth domain and high-density skyrmion state at zero field and room temperature. When a sufficient magnetic field of $H_2 = 1000$ Oe is applied and then removed, a single domain is formed [Fig. 4(b)]. Similarly, the labyrinth domains appear after injecting an electric current pulse with density of $J = 3.84 \times 10^8$ A/m^2 [Fig. 4(c)]. When a current with density of $J = 3.84 \times 10^8$ A/m^2 and a perpendicular magnetic field of $H_1 = 60$ Oe have been simultaneously applied, high-density skyrmions are formed at zero field and room temperature [Fig. 4(a)]. The created high-density skyrmions are proved to be robust after several days in the field-free environment (in a vacuum vessel) at room temperature. The direct observation of transformation between these three states has been recorded as *in situ* videos (videos S1–S4, supplementary information). High-density skyrmion state can be directly transformed from the other states including single domain or labyrinth domain state when the special magnetic field and current density have been applied. The skyrmion density at zero field is tunable by tailoring magnetic field strengths with the same current density. Therefore, we demonstrate that the multi-state of magnetic domains can be reliably switched with each other through the use of the specific current pulse and magnetic field. It should be noted that the multi-state domain is different from the concept of "multi-state" magnetization, which refers to the multilevel magnetization states during the reversal process.[38] The manipulation method can be extended to other SAFs with suitable PMA, enabling the multi-state interconversion of magnetic domains. On the other hand, the multistate domain transformation can also be realized in the $[Co/Pt]_4/NiO/[Co/Pt]_4$ with FM coupling.[30] Therefore, such interconversion may be closely related to the IEC in Hall balance so that the robust multi-state domains can be stabilized at zero field and room temperature, which will be explored in detail.

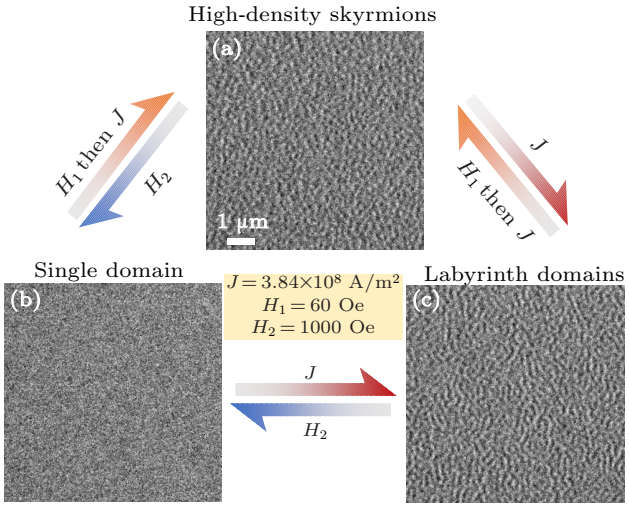


Fig. 4. Direct transformation of the three magnetic domain states at zero field and room temperature after manipulation under specific conditions. (a) Non-volatile high-density skyrmion state after applying a current density of $J = 3.84 \times 10^8$ A/m^2 under a constant perpendicular field of $H_1 = 60$ Oe. (b) Single domain state after being saturated at $H_2 = 1000$ Oe. (c) Labyrinth domain state after applying a current density of $J = 3.84 \times 10^8$ A/m^2. The scale bar is 1 μm.

4. Conclusion

In summary, the generation of magnetic domain structures together with their tunable behavior by the electromagnetic coordinated method has been demonstrated in the Hall balance. The transformation from the single domain state to labyrinth domains by applying the electric current is observed directly using LTEM. The topological skyrmions are generated via applying the electric current under a relatively small perpendicular magnetic field and can be stabilized at zero field and room temperature. Remarkably, non-volatile multi-state switching of magnetic textures can be realized after electromagnetic coordinated manipulation. The discovery of a tunable magnetic domain state in Hall balance provides key data for the fascinating mechanism of the electric current with different spin configurations and will shed light on its functionality as an excellent candidate in further spintronic devices.

Acknowledgments

This work was supported by the Science Center of the National Science Foundation of China (Grant No. 52088101), the National Natural Science Foundation of China (Grant Nos. 11874408, 52130103, 51901025, and 11904025), the Strategic Priority Research Program of the Chinese Academy of Sciences (Grant No. XDB33030100), and the Youth Innovation Promotion Association of Chinese Academy of Sciences (Grant No. CAS Y201903).

References

[1] Rossler U K, Bogdanov A N and Pfleiderer C 2006 *Nature* **442** 797
[2] Muhlbauer S, Binz B, Jonietz F, Pfleiderer C, Rosch A, Neubauer A, Georgii R and Boni P 2009 *Science* **323** 915
[3] Fert A, Cros V and Sampaio J 2013 *Nat. Nanotechnol.* **8** 152
[4] Tomasello R, Martinez E, Zivieri R, Torres L, Carpentieri M and Finocchio G 2014 *Sci. Rep.* **4** 6784
[5] Wang Y, Wang L, Xia J, Lai Z X, Tian G, Zhang X C, Hou Z P, Gao X S, Mi W B, Feng C, Zeng M, Zhou G F, Yu G H, Wu G H, Zhou Y, Wang W H, Zhang X X and Liu J M 2020 *Nat. Commun.* **11** 3577
[6] Münzer W, Neubauer A, Adams T, Mühlbauer S, Franz C, Jonietz F, Georgii R, Böni P, Pedersen B, Schmidt M, Rosch A and Pfleiderer C 2010 *Phys. Rev. B* **81** 041203
[7] Yu X Z, Onose Y, Kanazawa N, Park J H, Han J H, Matsui Y, Nagaosa N and Tokura Y 2010 *Nature* **465** 901
[8] Yu X Z, Kanazawa N, Onose Y, Kimoto K, Zhang W Z, Ishiwata S, Matsui Y and Tokura Y 2011 *Nat. Mater.* **10** 106
[9] Heinze S, von Bergmann K, Menzel M, Brede J, Kubetzka A, Wiesendanger R, Bihlmayer G and Blügel S 2011 *Nat. Phys.* **7** 713
[10] Pollard S D, Garlow J A, Yu J W, Wang Z, Zhu Y M and Yang H 2017 *Nat. Commun.* **8** 14761
[11] He M, Li G, Zhu Z Z, Zhang Y, Peng L C, Li R, Li J Q, Wei H X, Zhao T Y, Zhang X G, Wang S G, Lin S Z, Gu L, Yu G Q, Cai J W and Shen B G 2018 *Phys. Rev. B* **97** 174419
[12] He M, Peng L C, Zhu Z Z, Li G, Cai J W, Li J Q, Wei H X, Gu L, Wang S G, Zhao T Y, Shen B G and Zhang Y 2017 *Appl. Phys. Lett.* **111** 202403
[13] Yu G Q, Upadhyaya P, Li X, Li W Y, Kim S K, Fan Y B, Wong K L, Tserkovnyak Y, Amiri P K and Wang K L 2016 *Nano Lett.* **16** 1981
[14] Moreau-Luchaire C, Mouta S C, Reyren N, Sampaio J, Vaz C A, Van Horne N, Bouzehouane K, Garcia K, Deranlot C, Warnicke P, Wohlhuter P, George J M, Weigand M, Raabe J, Cros V and Fert A 2016 *Nat. Nanotechnol.* **11** 444

[15] Soumyanarayanan A, Raju M, Gonzalez Oyarce A L, Tan A K C, Im M Y, Petrovic A P, Ho P, Khoo K H, Tran M, Gan C K, Ernult F and Panagopoulos C 2017 *Nat. Mater.* **16** 898

[16] Zhou Y and Ezawa M 2014 *Nat. Commun.* **5** 4652

[17] Iwasaki J, Mochizuki M and Nagaosa N 2013 *Nat. Nanotechnol.* **8** 742

[18] Sampaio J, Cros V, Rohart S, Thiaville A and Fert A 2013 *Nat. Nanotechnol.* **8** 839

[19] Lin S Z 2016 *Phys. Rev. B* **94** 020402

[20] Romming N, Hanneken C, Menzel M, Bickel J E, Wolter B, von Bergmann K, Kubetzka A and Wiesendanger R 2013 *Science* **341** 636

[21] Buttner F, Lemesh I and Beach G S D 2018 *Sci. Rep.* **8** 4464

[22] Thiaville A, Rohart S, Jué É, Cros V and Fert A 2012 *Europhys. Lett.* **100** 57002

[23] Litzius K, Lemesh I, Kruger B, Bassirian P, Caretta L, Richter K, Buttner F, Sato K, Tretiakov O A, Forster J, Reeve R M, Weigand M, Bykova L, Stoll H, Schutz G, Beach G S D and Klaui M 2017 *Nat. Phys.* **13** 170

[24] Jiang W J, Zhang X C, Yu G Q, Zhang W, Wang X, Jungfleisch M B, Pearson J E, Cheng X M, Heinonen O, Wang K L, Zhou Y, Hoffmann A and te Velthuis S G E 2017 *Nat. Phys.* **13** 162

[25] Barker J and Tretiakov O A 2016 *Phys. Rev. Lett.* **116** 147203

[26] Jungwirth T, Marti X, Wadley P and Wunderlich J 2016 *Nat. Nanotechnol.* **11** 231

[27] Zhang J Y, Yang G, Wang S G, Liu J L, Wang R M, Amsellem E, Kohn A and Yu G H 2015 *Appl. Phys. Lett.* **106** 152401

[28] Zhang S L, Liu Y, Collins-Mclntyre L J, Hesjedal T, Zhang J Y, Wang S G and Yu G H 2013 *Sci. Rep.* **3** 2087

[29] Zhang X C, Zhou Y and Ezawa M 2016 *Nat. Commun.* **7** 10293

[30] Zhang J Y, Zhang Y, Gao Y, Zhao G P, Qiu L, Wang K Y, Dou P W, Peng W L, Zhuang Y, Wu Y F, Yu G Q, Zhu Z Z, Zhao Y C, Guo Y Q, Zhu T, Cai J W, Shen B G and Wang S G 2020 *Adv. Mater.* **32** 1907452

[31] Chen R Y, Gao Y, Zhang X C, Zhang R Q, Yin S Q, Chen X Z, Zhou X F, Zhou Y J, Xia J, Zhou Y, Wang S G, Pan F, Zhang Y and Song C 2020 *Nano Lett.* **20** 3299

[32] Peng L C, Zhang Y, He M, Ding B, Wang W H, Tian H F, Li J Q, Wang S G, Cai J W, Wu G H, Liu J P, Kramer M J and Shen B G 2017 *Npj Quantum Materials* **2** 30

[33] Peng L C, Zhang Y, He M, Ding B, Wang W H, Li J Q, Cai J W, Wang S G, Wu G H and Shen B G 2018 *J. Phys.-Condens. Mat.* **30** 065803

[34] Yang S, Moon K W, Ju T S, Kim C, Kim H J, Kim J, Tran B X, Hong J I and Hwang C 2021 *Adv. Mater.* **33** 2104406

[35] Yang M Y, Cai K M, Ju H L, Edmonds K W, Yang G, Liu S, Li B H, Zhang B, Sheng Y, Wang S G, Ji Y and Wang K Y 2016 *Sci. Rep.* **6** 20778

[36] Cai K M, Yang M Y, Ju H L, Wang S M, Ji Y, Li B H, Edmonds K W, Sheng Y, Zhang B, Zhang N, Liu S, Zheng H Z and Wang K Y 2017 *Nat. Mater.* **16** 712

[37] Cao Y, Sheng Y, Edmonds K W, Ji Y, Zheng H Z and Wang K Y 2020 *Adv. Mater.* **32** 1907929

[38] Cao Y, Rushforth A, Sheng Y, Zheng H Z and Wang K Y 2019 *Adv. Funct. Mater.* **29** 1808104